Spin-Peierls Ground States and Frustration in a Multiband Peierls-Hubbard Model

H. Röder,[1] A. R. Bishop,[2] and J. Tinka Gammel[3]
[1] *Physikalishes Institüt, Universität Bayreuth, W-8580 Bayreuth, Federal Republic of Germany*
[2] *Theoretical Division, Los Alamos National Laboratory, Los Alamos, New Mexico 87545*
[3] *Materials Research Branch, NCCOSC RDT&E Division (NRaD), San Diego, California 92152-5000*
(Received 20 November 1992)

We discuss the consequences of including both electron-phonon and electron-electron couplings in multiband models, focusing on numerical studies of a one-dimensional two-band model in the intermediate regime for both coupling strengths. Spin-Peierls as well as long-period, frustrated ground states are identified, reminiscent of those found in axial next-nearest-neighbor Ising models. We speculate on experimentally observable signatures of this rich phase diagram.

PACS numbers: 75.30.Fv, 64.70.Rh, 71.38.+i, 71.45.Lr

Multiband and multiorbital models have recently been much studied, primarily due to their relevance for high-temperature superconductors (HTS) [1]. At stoichiometry, such models can exhibit interesting and unusual ground states, such as electron-phonon (e-ph) driven incommensurate long-period or superlattice phases [2]. Here we show that a one-dimensional (1D), two-band model with competing electron-electron (e-e) and e-ph interactions also exhibits at stoichiometry qualitatively new *magnetic* behavior, namely, frustrated or spin-Peierls phases in the intermediate regime between the strongly electron-electron (e-e) correlated antiferromagnetic limit and the strongly e-ph correlated large lattice distortion limit. Similar complex phases are found in, e.g., axial next-nearest neighbor-Ising (ANNNI) models [3].

Considerable effort has gone into solving effective one-band models. For dominant e-e interactions Zhang and Rice [4] derived for HTS, due to the separation of energy scales, an effective one-band t-J Hamiltonian. Imada [5] suggested that inclusion of an e-ph dependent effective spin interaction J is crucial, as it opens a spin gap, important for singlet superconductivity. Here we stress phenomena which extend to several interaction forms and parameter ranges, and for which keeping the *full* two-band model with *both* e-e and e-ph interactions is essential.

We study the 1D, two-band, 3/4-filled, tight-binding Peierls-Hubbard Hamiltonian developed [6, 7] to model an interesting class of 1D compounds—halogen-bridged transition-metal linear chain complexes (MX chains)—which exhibit tunable behavior ranging from antiferromagnetic or spin-density wave to charge-density wave (CDW) to semimetallic. This same model can be considered as follows: a model of CuO chains; a 1D analog of the models used for CuO_2 planes in HTS [8]; a 3/4-filled analog of the the organic conductor polyacetylene; a model for charge-transfer salts such as TTF-TCNQ; or a model of neutral-ionic transitions [9]. If one considers the two orbitals to be on the same site, it is also related to the Kondo Hamiltonian used to describe heavy fermions. This model yields quantitative fits for the MX chain compounds to a variety of experimental data (optical absorption, Raman spectra, ESR, etc.) [6, 7].

Our 1D, two-band, Peierls-Hubbard Hamiltonian is [6, 7]

$$H = \sum_{l,\sigma}\{(-t_0+\alpha\delta_l)(c^\dagger_{l,\sigma}c_{l+1,\sigma}+c^\dagger_{l+1,\sigma}c_{l,\sigma}) + [\epsilon_l-\beta_l(\delta_l+\delta_{l-1})]c^\dagger_{l,\sigma}c_{l,\sigma}\} + \sum_l\{U_l c^\dagger_{l,\uparrow}c_{l,\uparrow}c^\dagger_{l,\downarrow}c_{l,\downarrow}+\tfrac{1}{2}K(\delta_l-a_1)^2+P\delta_l\}, \quad (1)$$

where $c^\dagger_{l,\sigma}$ creates an electron at site l with spin σ. M (d_{z^2}) and X (p_z) Wannier orbitals are situated on even and odd sites, respectively. Each M_2X_2 unit cell has 6 electrons, or 3/4 band filling. Parameters are the on-site energy (ϵ_l, $\epsilon_M=-\epsilon_X=e_0\geq 0$), electron hopping ($t_0$), on-site ($\beta_M,\beta_X$) and inter-site ($\alpha$) e-ph coupling, on-site e-e repulsion (U_M, U_X), and pressure P. a_1 is the natural length of the effective M-X spring K [10]. δ_l, the relative displacement of sites l and $l+1$, is determined by minimizing the total energy. We have used both Hartree-Fock and exact diagonalization to study this model [6].

For $e_0 \gg 0$, one starting point for interpreting the effects of e-e and e-ph couplings is an effective 1/2-filled, one-band model focusing on the M d_{z^2} orbitals [11]. For zero e-e correlations, when the on-site e-ph coupling $\beta^{\rm eff}_{\rm 1B}$ dominates, the ground state exhibits X-sublattice distortion with an accompanying CDW on the M sublattice (CDW phase). The case is reversed when the intersite e-ph coupling $\alpha^{\rm eff}_{\rm 1B}$ dominates: X-CDW and M-sublattice distortion [bond-order-wave (BOW) phase]. Typical e-ph phenomena (phonon softening, solitons, etc.) are found [11]. The full two-band model leads to qualitative modifications: the BOW phase is removed [6], and upon doping localized intrinsic defects now exhibit electron/hole asymmetry [12] and local charge, spin, and/or lattice-distortion character [6, 7], e.g., local lattice distortion around "magnetic" polarons in an antiferromagnet such as NiCl or NiBr [7]. Near phase boundaries, even at low defect concentration, strong modification of the background (stoichiometric "ground state") also occurs [13]. Our focus here is on intermediate to large e-e correlations (large U_M), where in the 1D, one-band limit one expects

TABLE I. The $a=a_1=0$ constant volume period-4 phases, occupancies, distortions, energies, and effective antiferromagnetic spin correlations J in the $t_0\to 0$ limit. Here $t=t_0/e_0$, $u_{m,x}=U_{M,X}/e_0$, $b_{m,x}=\beta_{M,X}(Ke_0)^{-1/2}$, and $d_X(d_M)$ are dimensionless $X(M)$ sublattice distortion order parameters, $\delta(l)=d_X(e_0/K)^{1/2}(\cos\frac{\pi}{2}l-\sin\frac{\pi}{2}l)-d_M(e_0/K)^{1/2}(\cos\frac{\pi}{2}l+\sin\frac{\pi}{2}l)$. E_T is the total energy of the N site chain using periodic boundary conditions. The change in average M-X bond length a, $a=\sum_l \delta_l/N$, and the pressure P are related by $\partial E_T/\partial P=Na$, yielding $P=K(a_1-a+D)$, where $D=\sum_{l,\sigma}\langle 2\beta_l c^\dagger_{l,\sigma}c_{l,\sigma}-\alpha(c^\dagger_{l,\sigma}c_{l+1,\sigma}+c^\dagger_{l+1,\sigma}c_{l,\sigma})\rangle/NK$.

Phase	$X\,M\,X\,M$	d_M	d_X	$D\sqrt{\frac{K}{e_0}}$	$2E_T/(e_0N)$	$J^{\rm eff}/e_0$
MAF	$\Uparrow-\uparrow-\Uparrow-\downarrow-$	0	0	$2b_x+b_m$	u_x-1	$\frac{J_{MM}}{e_0}=\frac{t^4(4u_m-u_x+4)}{2u_m(u_m-u_x+2)^2(2u_m-u_x+4)}$
XAF	$\uparrow-\Uparrow-\downarrow-\Uparrow-$	0	0	b_x+2b_m	u_m+1	$\frac{J_{XX}}{e_0}=\frac{t^4(4u_x-u_m-4)}{2u_x(u_x-u_m-2)^2(2u_x-u_m-4)}$
MXP	$\uparrow=\downarrow-\Uparrow\cdots\Uparrow-$	$\frac{1}{2}b_m$	$\frac{1}{2}b_x$	$3\frac{b_x+b_m}{2}$	$\frac{u_x+u_m}{2}-\frac{b_x^2+b_m^2}{4}$	$\frac{J_{MX}}{e_0}=\frac{t^2(u_m+u_x)}{(u_x-2+b_x^2-b_m^2)(u_m+2-b_x^2+b_m^2)}$
CDW	$\Uparrow=\bullet=\Uparrow-\Uparrow-$	b_m	0	$2b_x+b_m$	$u_x+\frac{1}{2}u_m-1-b_m^2$	$\cdots$
BOW	$\bullet=\Uparrow-\Uparrow-\Uparrow=$	0	b_x	b_x+2b_m	$\frac{1}{2}u_x+u_m+1-b_x^2$	$\cdots$

a spin-Peierls phase with an effective antiferromagnetic coupling between M sites [4, 14, 15].

To understand the consequences of e-e correlations for our multiband model, we first examine the zero-hopping limit [16]. The period-4 phases for $t_0=\alpha=0$ are listed in Table I. The phase diagram for parameter values near the CDW/antiferromagnetic crossover, relevant to MI or NiX materials, is shown in Fig. 1. The phase diagram is more complex for $U_X,|\beta_X|\gtrsim U_M,|\beta_M|$ and/or $\beta_X/\beta_M>0$, where the hybridization-driven competition is most effective. For $t_0=0$ and U_M dominant, the lower, X-like band is full and nonmagnetic, while the upper, M-like band is 1/2 full with one electron per M site and uncorrelated spins. For $t_0\neq 0$, as in the one-band case, there is an effective antiferromagnetic coupling between spins on neighboring metal sites, J_{MM}, which drives antiferromagnetic order which competes with band splitting driven by the on-site e-ph coupling β. However, hybridization between the two bands also occurs: as the lower band is not completely full there are effective antiferromagnetic couplings between neighboring X sites, J_{XX}, and between M and X sites, J_{MX}, not present in one-band models [17]. In fact, when the splitting due to β is on the order of U and e_0, the antiferromagnetic state with neighboring M-X pairs singly occupied can become the ground state; see Fig. 1. This implies, in contrast to the one-band case, that the combination of e-e and e-ph coupling in the two-band model drives, in addition to the nonmagnetic CDW and BOW phases, three (competing) spin-Peierls phases: one on the X sublattice (XAF), one on the M sublattice (MAF), and one involving M-X pairs and large lattice distortion (MXP). Since J_{MM}, J_{XX}, and J_{MX} are all antiferromagnetic couplings ($J>0$), they cannot all be simultaneously satisfied and the system is frustrated, as illustrated in Fig. 2. The expressions for the J from fourth-order perturbation theory in t_0 are listed in Table I. When only one of the J's dominates, one can numerically check these estimates by comparing the energies of the singlet and triplet ground states (at fixed lattice distortion). Figure 3 shows good agreement for small t_0. Note that the CDW phase has an entirely e-ph driven anitferromagnetic component: even when the $X(M)$-sublattice distortion is large, some residual $M(X)$-sublattice magnetization remains.

For parameters where the lattice distortion is large and driven by the on-site e-ph coupling β, and/or the Hubbard U terms are large, Fig. 1 is close to the actual phase diagram. Figure 4 presents exact diagonalization results for such a case. As U_M increases (lattice distortion decreases), we observe a sharp transition from M-M charge coupling (CDW) to M-X spin coupling (MXP) to M-M spin coupling (MAF), in agreement with the $t_0=0$ results.

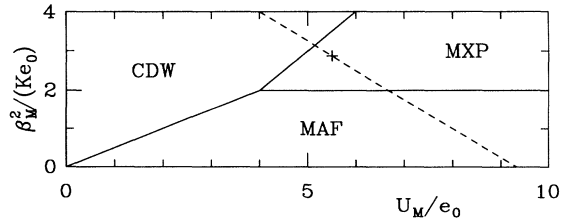

FIG. 1. $t_0=0$ phase diagram, infinite chain: $\beta_X/\beta_M=-1$, $U_X/U_M=1$. Figures 3 (+) and 4 (---) parameters are shown. Varying pressure corresponds to a line through the origin.

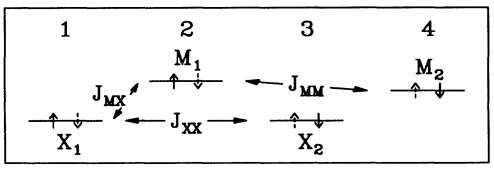

FIG. 2. Schematic energy level diagram in the strongly correlated limit showing frustration of the effective antiferromagnetic couplings due to the partial occupancy of the low-lying X orbitals induced by M-X hybridization.

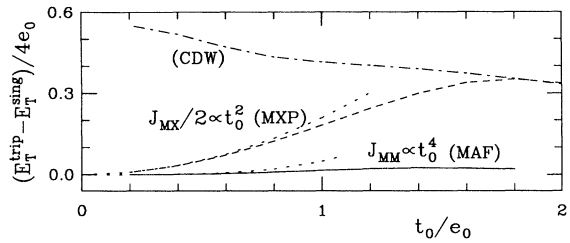

FIG. 3. Exact diagonalization, 16-site ring: t_0 dependence of the difference in singlet and triplet energies for the CDW, MXP, and MAF phases at the + in Fig. 1. For $t_0 \ll U_M$, this corresponds to excitations of the effective spin Hamiltonian $H = 4JS_i^z S_{i+j}^z$ ($4J_{MM}$, MAF phase; $2J_{MX}$, MXP phase); in the CDW phase this reflects the Peierls gap. The dotted lines are perturbative expressions (Table I).

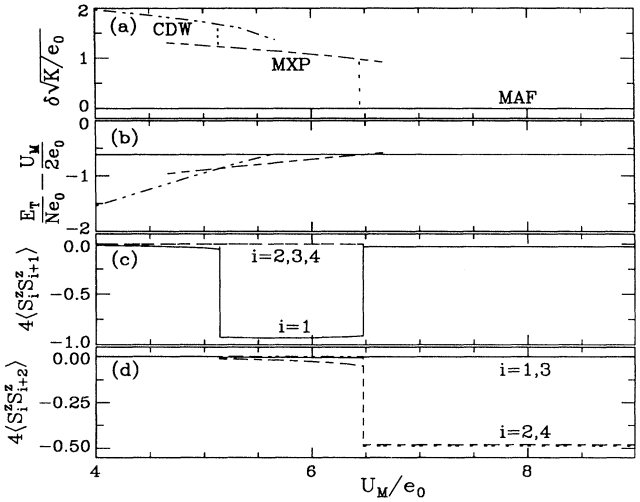

FIG. 4. Exact diagonalization, 16-site ring: (a) lattice distortion amplitude, (b) total energy E_T, and (c) NN and (d) NNN spin correlations as a function of U_M/e_0 on the line in Fig. 1 for MAF, CDW, and MXP phases at $t_0/e_0=0.5$. For finite systems lattice distortion strongly pins competing phases, thus we can follow them across phase boundaries.

For larger t_0, the couplings change more smoothly, and charge disproportionation, M-X spin coupling, and M-M spin coupling coexist, with the phase of the lattice distortion passing from CDW through MXP to BOW as the amplitude goes to zero. For large t_0, even for $U_M=0$, the CDW phase shows a strong tendency towards antiferromagnetic order, but driven by valence fluctuations.

The crossover between the period-4 CDW and MAF phases is accompanied by long-period superlattice phases [18] when $|\beta_X/\beta_M|>1$ or the *intersite* e-ph coupling α is large. We have completed only preliminary evaluation of the long-period region of the phase diagram, as the many competing metastable states significantly complicate analysis. Superlattices may be viewed as ordered arrays of discommensuration defects with respect to nearby commensurate (period-4) order. Considering the effective J's discussed above, it may be natural to view such states in terms of ANNNI-like models [3, 5, 14] where nearest and longer range couplings compete leading to frustration and associated complexity phenomena—multi-time-scale relaxation, hysteresis, metastability, etc.

In the context of the MX class and similar 1D systems, it will be particularly interesting to investigate materials in, or near, this crossover regime, and to further control the crossover with pressure, magnetic field, doping, impurities, etc. In terms of doping into such phases, especially near phase boundaries, besides the usual plethora of doping and photoinduced nonlinear excitations (solitons, polarons, bipolarons, and excitons [6, 7, 9, 11]), a dopant-induced *global* phase transition may exist [13] and novel pairing mechanisms are anticipated [4, 5, 14, 19]. We expect the complicated spin and charge character of these unusual broken-symmetry states to be experimentally accessible with appropriate probes of spin, charge, and lattice structure (frequency dependent conductivity, susceptibility, precise x-ray analysis, ENDOR, etc.)—in fact, in the weak CDW system PtI unexpectedly strong diamagnetism has already been reported [20], which may be the smoking gun. *Doping* into this complex regime should be highly sensitive to the softness and competitions of the phases: this is an excellent regime to study pairing tendencies and metallization, or develop device applications [21].

In the context of antiferromagnetic-based HTS materials the role of e-ph coupling is increasingly appreciated [1]. Tuning e_0, t_0, U_M, and U_X in the Hamiltonian (1) is a 1D analog of theoretical discussions in 2D which focus on the p-d hybridization in HTS materials. There, as here, these parameters determine the broken symmetry (if any) of the ground state, and the nature of electron or hole doping into those states. The same CDW/antiferromagnet competition occurs and the nominal filling is effectively the same in both MX and oxide HTS materials—3/4 filling of two bands and 5/6 filling of three bands, respectively. Furthermore, both antiferromagnetic and CDW HTS compounds exist (e.g., based on $LaCu_2O_4$ and $BaBiO_3$), much as for MX compounds (e.g., NiCl and PtCl, respectively). Inclusion of e-ph coupling in 2D leads to effects similar to those reported here: a 2D α-driven long-period phase has recently been found [19]. As in the 1D case, in addition to complex stoichiometric phases, upon doping unusual pairing mechanisms are anticipated [4, 5, 14, 19] and generalized polaronic or "bag" states are predicted [19] with a rapid crossover from a Zhang-Rice singlet [4] to a covalent molecular singlet and with local coexistence of spin and charge—e.g., strong *local* lattice distortion in a strongly magnetic background. Doping and photodoping spectroscopy [22] support this prediction. Spontaneous

separation of spin and charge driven by the competition between magnetism and covalency is also predicted [19] upon doping into globally complex ground states analogous to those discussed above.

We stress that the 1D, two-band, Peierls-Hubbard Hamiltonian studied is representative of a very large variety of low-D electronic materials with a richness both of possible ground states and of consequences of doping into these states, especially near phase boundaries. We are exploiting this richness via a systematic "making-measuring-modeling" approach to the MX class of 1D compounds, which are realizations of this Hamiltonian spanning the range of complex broken symmetry ground states. We believe that experimental investigations of the template [23], pressure, and magnetic field dependent behavior of pure, disordered, and doped MX materials in the lattice-distortion/antiferromgnetic crossover regime (PtI, NiBr, or their mixed-metal or -halide analogs) will continue to yield interesting insights into the nature of intrinsically multiband effects and the competition between e-e and e-ph interactions.

We thank X. Z. Huang, E. Y. Loh, Jr., A. Saxena, J. Shi, and K. Yonemitsu for important discussions. A.R.B. was supported by the U.S. DOE, H.R. by the Deutsche Forschungsgemeinschaft through SFB 213, and J.T.G. by a National Research Council-NRaD Research Associateship through a grant from the ONR. Supercomputer access was through the Advanced Computing Laboratory at LANL. H.R. and J.T.G. are grateful to the hospitality of LANL, where this work was begun.

[1] *Lattice Effects in High T_c Superconductors*, edited by Y. Bar-Yam, T. Egami, J. Mustre-deLeon, and A.R. Bishop (World Scientific, Singapore, 1992).
[2] I. Batistić, J.T. Gammel, and A.R. Bishop, Phys. Rev. B **44**, 13 228 (1991).
[3] W. Selke and M.E. Fisher, Phys. Rev. B **20**, 257 (1979); P. Bak and J. v. Bohm, Phys. Rev. B **21**, 5297 (1980).
[4] F.C. Zhang and T.M. Rice, Phys. Rev. B **37**, 3759 (1988); **41**, 2560 (1990).
[5] M. Imada, J. Phys. Soc. Jpn. **60**, 1877 (1991); **61**, 423 (1992); (unpublished).
[6] J.T. Gammel *et al.*, Phys. Rev. B **45**, 6408 (1992).
[7] S.M. Weber-Milbrodt *et al.*, Phys. Rev. B **45**, 6435 (1992).
[8] J.T. Gammel *et al.*, Physica (Amsterdam) **163B**, 458 (1990).
[9] A. Painelli and A. Girlando, Synth. Met. **29**, F181 (1989); X.Z. Huang *et al.* (unpublished).
[10] Longer-range Coulomb effects have been investigated [9], we tested NNN hopping and springs, and α and β may be viewed as expansions of longer-range Fröhlich terms. Such extensions do not change our qualitative discussion.
[11] D. Baeriswyl and A.R. Bishop, Phys. Scr. **T19**, 239 (1987); K. Nasu, J. Phys. Soc. Jpn. **50**, 235 (1981).
[12] J.T. Gammel *et al.*, Phys. Rev. B **42**, 10 566 (1990).
[13] J. Reichl (unpublished); S. Marianer (unpublished).
[14] V.J. Emery and G. Reiter, Phys. Rev. B **38**, 11 938 (1988); **41**, 7247 (1990).
[15] J. Shi, R. Bruinsma, and A.R. Bishop, Phys. Rev. B (to be published).
[16] Decoupled limits, e.g., $X{=}M{=}X$ trimers and M monomers for the CDW phase, agree with the $t{=}0$ analysis.
[17] While effective one-band t-J models may be valid in both the MAF and MXP phases—e.g., using M-X singlets [4] potentially with an e-ph dependent J [5]—to model the MAF/MXP crossover would require distinguishing between M-$X{=}2$-$\uparrow$ and $\uparrow$-2, and thus a multiorbital model.
[18] Intermediate phases, driven by competitions between t_0, β, α, long-range Coulomb fields, and/or frustration of the effective J's, can be period-4 (commensurate) or long period. The incommensurate large-β phase [2] differs from the frustration driven, magnetic long-period phase discussed here (or in 2D for large α in Ref. [19]).
[19] K. Yonemitsu and A.R. Bishop, Phys. Rev. B **45**, 5530 (1992); K. Yonemitsu *et al.* (unpublished); in *Lattice Effects in High T_c Superconductors* (Ref. [1]).
[20] M. Haruki and P. Wachter, Phys. Rev. B **43**, 6273 (1991).
[21] L.A. Worl *et al.*, J. Phys. C **4**, 10 237 (1992); A. Saxena *et al.*, Synth. Met. **54**, 385 (1993).
[22] E.g., G. Yu *et al.*, Phys. Rev. Lett. **67**, 2581 (1991); G.A. Thomas *et al.*, Phys. Rev. Lett. **67**, 2906 (1991).
[23] In mixed MXX' crystals, the MX' phase may be controlled by the lattice constant of the host MX crystal [B. Scott *et al.*, Synth. Met. (to be published)].